ORIGINAL RESEARCH

Simultaneous Real-Time Detection of Pregnancy-Associated Plasma Protein-a and -A2 Using a Graphene Oxide-Based Surface Plasmon Resonance Biosensor

Shi-Yuan Fan [ID][1]
Nan-Fu Chiu [ID][2]
Chie-Pein Chen[1,3]
Chia-Chen Chang[4]
Chen-Yu Chen [ID][1,3]

[1]Department of Obstetrics and Gynecology, Mackay Memorial Hospital, Taipei, Taiwan; [2]Institute of Electro-Optical Science and Technology, National Taiwan Normal University, Taipei, Taiwan; [3]Department of Medicine, Mackay Medical College, New Taipei City, Taiwan; [4]Department of Medical Biotechnology and Laboratory Science, Chang Gung University, Taoyuan City, Taiwan

Background: Pregnancy-associated plasma protein-A and -A2 (PAPP-A and -A2) are principally expressed in placental trophoblasts and play a critical role in the regulation of fetal and placental growth. PAPP-A2 shares 45% amino acid similarity with PAPP-A. This study aimed to investigate the efficacy of real-time detection of PAPP-A and PAPP-A2 using a novel surface plasmon resonance (SPR) biosensor based on graphene oxide (GO).

Methods: Traditional SPR and GO-based SPR chips were fabricated to measure PAPP-A and PAPP-A2 concentrations. We compared SPR response curves of PAPP-A and PAPP-A2 between traditional SPR and GO-SPR biosensors. We also performed interference tests and specificity analyses among PAPP-A, PAPP-A2, and mixed interference proteins.

Results: The time to detect PAPP-A and PAPP-A2 was about 150 seconds with both traditional SPR and GO-SPR biosensors. Approximately double SPR angle shifts were noted with the GO-SPR biosensor compared to the traditional SPR biosensor at a PAPP-A and PAPP-A2 concentration of 5 μg/mL. The limit of detection of the GO-SPR biosensor was as low as 0.5 ng/mL for both PAPP-A and PAPP-A2. Interference testing revealed that almost all of the protein bonded on the GO-SPR biosensor with anti-PAPP-A from the mixture of proteins was PAPP-A, and that almost no other proteins were captured except for PAPP-A2. However, the SPR signal of PAPP-A2 (5.75 mdeg) was much smaller than that of PAPP-A (13.76 mdeg). Similar results were noted with anti-PAPP-A2, where almost all of the protein bonded on the GO-SPR biosensor was PAPP-A2. The SPR signal of PAPP-A (5.17 mdeg) was much smaller than that of PAPP-A2 (13.94 mdeg).

Conclusion: The GO-SPR biosensor could distinguish PAPP-A and PAPP-A2 from various mixed interference proteins with high sensitivity and specificity. It could potentially be used to measure PAPP-A and PAPP-A2 in clinical blood samples during pregnancy.

Keywords: pregnancy-associated plasma protein-A, pregnancy-associated plasma protein-A2, graphene oxide, surface plasmon resonance, biosensor

Introduction

Pregnancy-associated plasma protein-A (PAPP-A) is a 200 kDa zinc-binding metalloproteinase of the metzincin superfamily. PAPP-A circulates as a 500 kDa disulfide-bound complex with eosinophil major basic protein in pregnancy and as a 400 kDa homodimer outside pregnancy.[1] It is mainly produced by placental trophoblasts and is a critical protease that cleaves insulin-like growth factor binding protein-4 (IGFBP-4)

Correspondence: Chen-Yu Chen
Department of Medicine, Mackay Medical College, No. 46, Section 3, Zhongzheng Road, Sanzhi District, New Taipei City 252, Taiwan
Tel +886 2 2636 0303
Email f122481@mmh.org.tw

to release free insulin-like growth factors (IGFs). Cleavage of IGFBP-4 by PAPP-A occurs only in the presence of IGFs (IGF-dependent).[2] PAPP-A2 is a 220 kDa homologue of PAPP-A that shares 45% amino acid similarity with PAPP-A.[3] PAPP-A2 specifically cleaves IGFBP-5 to release IGFs but is not IGF-dependent. PAPP-A2 may therefore contribute to the same growth regulatory system but with different physiological functions than PAPP-A. Similar to PAPP-A, PAPP-A2 originates primarily from the placenta, but its expression is not limited to pregnancy.[4]

Both PAPP-A and PAPP-A2 participate in fetal growth and development by cleaving IGFBPs, which can increase IGF bioavailability and bioactivity.[5] PAPP-A and PAPP-A2 are secreted into the maternal circulation and have been shown to be valuable biomarkers for pregnancy-associated diseases. A low level of PAPP-A has been associated with a higher risk of fetal Down syndrome, low birth weight, preterm delivery, and maternal preeclampsia.[6,7] In contrast, a high level of PAPP-A2 has been associated with fetal Down syndrome, maternal pre-eclampsia and hypoxia due to impaired placentation.[8–10] In addition, an inverse association with birth weight has been reported between umbilical cord blood PAPP-A and PAPP-A2 levels, both of which are likely to be compensatory in IGF-related feedback mechanisms.[11] Therefore, both PAPP-A and PAPP-A2 are closely linked to regulation within the IGF system and have complex interactions.

In the past two decades, biosensors using surface plasmon resonance (SPR) response have been introduced. The physically phenomenon of SPR occurs at a metal boundary and involves electron charge oscillations with the wave vector propagating along the metal surface, and it can be excited by p-polarized light.[12] This technique has been used in chemical and biological fields with nanoparticle-derived SPR biosensors to detect biomolecules, in which measuring changes in the resonant angle can be used to determine the concentration of biomolecules of interest.[13–15] The advantages of SPR biosensors include real-time detection, fast measurement, label-free process, and easy preparation. Recently, SPR sensing based on various nanogold-based hybrid structures have been developed and shown promise.[16] The advancement of novel nanostructures is one of the important trends of nanobiotechnology.[17] Novel materials including graphene and its derivatives have been used to modify the propagation constant of surface plasmon polariton (SPP) and enhance the sensitivity of SPR biosensors.[18–22]

Graphene is an atomic-scale two-dimensional honeycomb crystal lattice of carbon atoms, and it is one of the most promising nanomaterials due to its excellent mechanical, electronic, chemical, and optical properties. Graphene oxide (GO), an oxidized graphene derivative, has a large surface area composed of an sp^2 within an sp^3 matrix and contains many functional carboxyl, hydroxyl, carbonyl, and epoxy groups. This unique structure means that GO has excellent hydrophilicity, amphiphilicity, surface functionalization, fluorescence quenching ability, and surface enhanced Raman scattering property.[23,24]

Previous studies have used SPR biosensors to measure PAPP-A[25–28] and PAPP-A2.[4,29,30] In our previous study, we demonstrated that a functionalized GO-based SPR biosensor had higher sensitivity, affinity and selective ability for PAPP-A2 than a traditional SPR biosensor.[30] However, no previous study has simultaneously measured both PAPP-A and PAPP-A2 using a GO-based SPR biosensor. In this study, we tried to measure both PAPP-A and PAPP-A2 simultaneously using a GO-based SPR biosensor, and further analyzed their cross-reactivity and complex interactions using this novel SPR biosensor. We also discussed further factors involved in the detection of PAPP-A and PAPP-A2 in terms of sensitivity, specificity, and affinity of the GO-SPR biosensor.

Materials and Methods
Preparation of Sensing Chip Procedures

The preparation of traditional SPR chips and GO-based SPR chips were based on and modified from our previous experiment.[19] Initially, a standard SPR thin film consisting of 47-nm thick gold (Au) and 2-nm thick chromium (Cr) deposited over a 0.17-mm thick glass (Initially, a standard SPR thin film consisting of 47-nm thick gold (Au) and 2-nm thick chromium (Cr) deposited over a 0.17-mm thick BK7 glass (refractive index, n= 1.5) substrate was prepared. The traditional SPR chip was generated by immersing the bare Au/Cr film in 10 mM 8-mercaptooctanoic acid (MOA, Sigma-Aldrich, USA) for 3 hrs. The MOA covalently bonded to the Au surface through a thiol linker, which resulted in a self-assembled monolayer and exposed carboxyl groups (Figure S1A).

The GO-SPR chip was prepared by immersing the bare Au/Cr film in 10 mM cystamine (Cys) (cystamine dihydrochloride, ≥ 98%, Alfa Aesar, USA) for 12 hrs. The Cys covalently bonded to the Au surface through a thiol linker, resulting in a monolayer and exposed amino groups. We

then added 1 mg/mL GO solution (Graphene Supermarket, USA) for 5 hrs, during which the carboxyl terminal of GO bound with the amino terminal of Cys, resulting in a strong amide covalent linkage (Figure S1B).

Figure S2A illustrates the molecular structure of a GO sheet containing many oxygen-containing functional groups including carboxyl, hydroxyl, carbonyl, and epoxy groups covalently bonded on the basal planes. The carboxyl groups were located at the edge of the GO sheet and the hydroxyl groups were located at the surface of the GO sheet. Scanning electron microscopy showed that the GO sheets formed an organic compound shell shape (Figure S2B).

Preparation of Protein Samples

PAPP-A and PAPP-A2 (APREST77476 and APREST73992, Sigma-Aldrich, USA) antigens were diluted to concentrations of 5000, 1000, 500, 100, 50, 10, and 0.5 ng/mL using 1X phosphate buffer saline (PBS, UniRegion Bio-Tech, Taiwan) in a volume of 250 μL. For the non-specific protein tests, we used different non-specific protein concentrations of 1 μg/mL each, and a volume of 250 μL for human cytokeratin 19 (CK-19, Novus Biologicals, USA), human serum albumin (HSA, Sigma-Aldrich, USA), human chorionic gonadotropin (hCG, Sigma-Aldrich, USA), and cancer antigen 19–9 (CA 19–9, MyBioSource, USA) proteins.
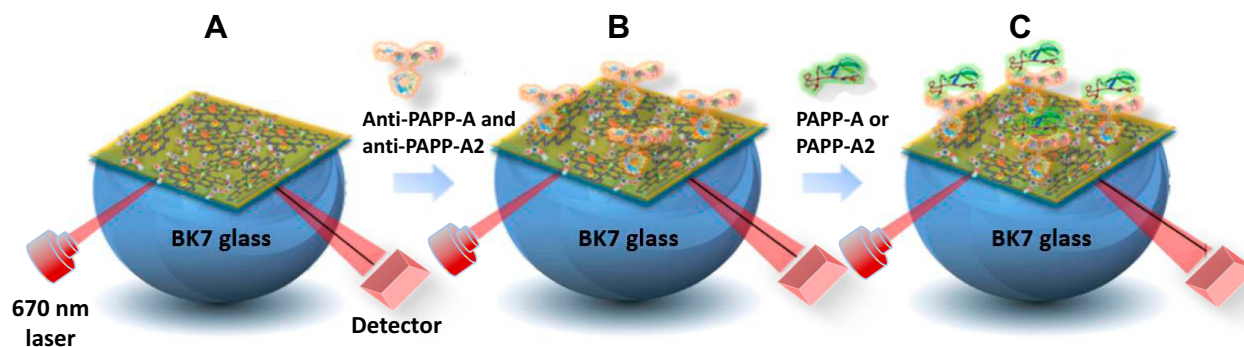
Immobilization of PAPP-a and PAPP-A2 Antibodies

The principle regarding the SPR biological experiment was to use a microfluidic system to capture antigens including PAPP-A and PAPP-A2 with the antibody-immobilized SPR chip (Figure 1). Before conducting the immobilization, 1% ethanol

(JT Baker, USA) was used to calibrate the GO based chip in the microfluidic system. The traditional SPR biosensors and GO-SPR biosensors were incubated in a mixture of 0.4 M 1-ethyl-3-(3-dimethylaminopropyl)-carbodiimide (EDC, Sigma-Aldrich, USA) and 0.1 M N-hydroxysuccinimide (NHS, Sigma-Aldrich, USA) that were diluted using deionized water at 4°C for 30 mins to activate the carboxyl groups on the surface of the GO sheets.[31] The carboxyl groups on the GO sheets facilitated immobilization of covalent bonding with the amino groups of anti-PAPP-A or anti-PAPP-A2 (HPA001667 and HPA018430, Sigma-Aldrich, USA) of 25 μg/mL, and the solutions were stored at 4°C for 3 hrs. These non-bonded carboxyl groups were then deactivated with 1 M ethanolamine hydrochloride (EA, Sigma-Aldrich, USA) at room temperature for 30 mins. Those free carboxyl groups exposed on the GO were blocked by EA to prevent the bonding of untargeted proteins. Finally, the remained carboxyl groups were blocked with 200 μg/mL bovine serum albumin (BSA, Sigma-Aldrich, USA) at room temperature for 10 mins.

Immunoassay for PAPP-a and PAPP-A2 Antigens

All SPR biological experiments were conducted using a dual-channel BI-3000 SPR instrument (Biosensing Instrument, Tempe, AZ, USA) with Kretschmann prism coupling. Figure 2 illustrates the microfluidic system for simultaneous detection of PAPP-A and PAPP-A2. Half of the biosensor was coated with anti-PAPP-A and the rest was coated with anti-PAPP-A2, and as a result the samples could pass through the region of both anti-PAPP-A and anti-PAPP-A2. PBS was poured over the sensing surface until a stable baseline was obtained. This step was followed by the introduction of

Figure 1 Illustration of a GO-SPR biosensor immobilized with anti-PAPP-A or anti-PAPP-A2 antibodies to assay PAPP-A or PAPP-A2 antigens.
Notes: (**A**) The configuration of GO-SPR biosensor. (**B**) Both anti-PAPP-A and anti-PAPP-A2 are immobilized on the GO-SPR biosensor. (**C**) Assaying PAPP-A or PAPP-A2 by the GO-SPR biosensor. BK7 is a standard glass (refractive index, n= 1.5) for all kinds of optics.
Abbreviations: GO, graphene oxide; SPR, surface plasmon resonance; PAPP-A, pregnancy-associated plasma protein-A; PAPP-A2, pregnancy-associated plasma protein-A2.
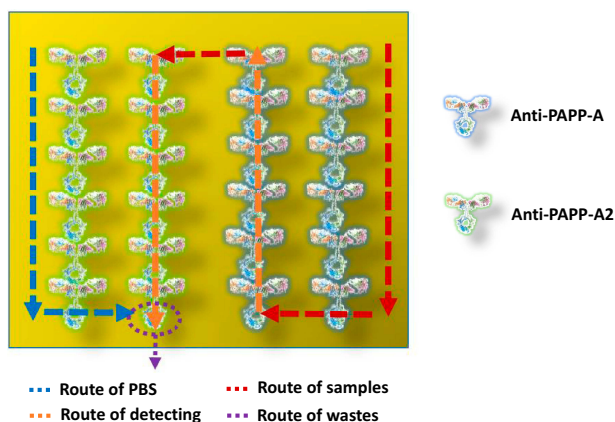
Figure 2 Illustration of the microfluidic system for simultaneous detection of PAPP-A and PAPP-A2.
Notes: Half of the biosensor is coated with anti-PAPP-A and the rest is coated with anti-PAPP-A2. The samples pass through the region of both anti-PAPP-A and anti-PAPP-A2.
Abbreviations: PAPP-A, pregnancy-associated plasma protein-A; PAPP-A2, pregnancy-associated plasma protein-A2; PBS, phosphate buffer saline.

various concentrations of antigen solutions onto the antibody-immobilized surface at a rate of 60 μL/min for 10 mins. Unbound antigens were then washed out with PBS for another 10 mins to achieve equilibrium. Three injections of 50 mM sodium hydroxide (NaOH, Sigma-Aldrich, USA) were used to remove proteins not covalently bonded to clean and regenerate the chip surfaces.

Mixed Sample Investigation and Interference Test with the GO-SPR Biosensor

We repeated the previous procedures of assaying PAPP-A and PAPP-A2 with the GO-SPR biosensor but changed the purified samples with mixed samples. The biological immunoassays and the other procedures including calibration and regeneration with 1% ethanol and 50 mM NaOH were identical to those performed above. For the interference test, we used a mixture containing four spiked proteins (CK-19, HSA, hCG, and CA 19–9) at a concentration of 1 μg/mL each, and a volume of 10 μL by mixing them with PAPP-A or PAPP-A2 (250 μL) in PBS. We added an extra 10 μL of 1 μg/mL PAPP-A2 in PAPP-A solution and 10 μL of 1 μg/mL PAPP-A in PAPP-A2 solution, and thus each mixed sample had a volume of 300 μL.

Results and Discussion
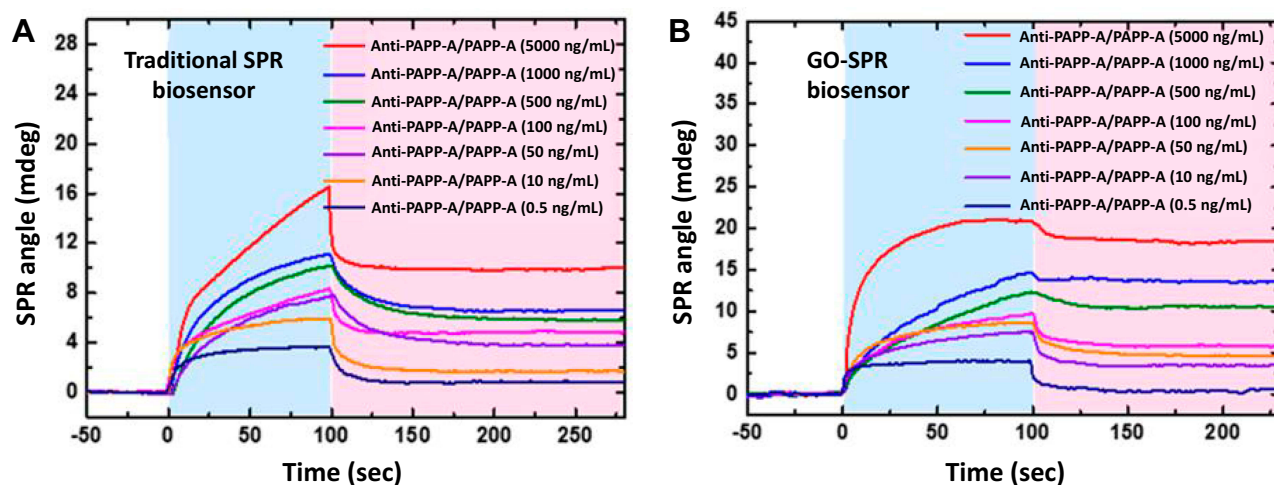### SPR Sensorgrams of PAPP-a and PAPP-A2

Figure 3A shows the results of assaying different concentrations of PAPP-A with the traditional SPR biosensor, and

Figure 3B shows the results of assaying PAPP-A with the GO-SPR biosensor. The white background indicates the period before the antibody-antigen reaction, the blue background indicates the antibody-antigen association, and the pink background indicates the antibody-antigen dissociation. SPR angle responses at a steady state versus different protein concentrations showed that the SPR angle shifts related to PAPP-A concentrations of 5000, 1000, 500, 100, 50, 10, and 0.5 ng/mL were 10.46, 6.41, 4.14, 2.99, 2.43, 1.89, and 0.93 millidegrees (mdegs), respectively, with the traditional SPR biosensor (Figure 3A), and 17.47, 13.14, 5.40, 3.41, 2.82, 2.26, and 0.82 mdegs, respectively, with the GO-SPR biosensor (Figure 3B).

Figure 4A shows the results of assaying different concentrations of PAPP-A2 with the traditional SPR biosensor, and Figure 4B shows the results of assaying PAPP-A2 with the GO-SPR biosensor. SPR angle shifts related to PAPP-A2 concentrations of 5000, 1000, 500, 100, 50, 10, and 0.5 ng/mL were 10.03, 6.65, 5.76, 4.78, 3.77, 1.72, and 0.84 mdegs, respectively, with the traditional SPR biosensor (Figure 4A), and 18.42, 13.52, 10.49, 5.75, 4.58, 3.44, and 0.69 mdegs, respectively, with the GO-SPR biosensor (Figure 4B).

Previous studies using traditional SPR biosensors to measure various types of antigen-antibody reactions of PAPP-A and PAPP-A2 have shown promising results (Table 1).[4,25-30] Mikkelsen et al[25] used SPR biosensors to assess the binding of pituitary adenylate cyclase-activating polypeptide type 1 (PAC1) receptor, a monoclonal single-chain fragment variable (scFv) antibody, to immobilize PAPP-A in the presence of calcium ions. They also investigated interactions between PAPP-A and recombinant antibodies PAC1-D8-scFv or PAC1-D8-mIgG2a in multiple animal species using SPR biosensors.[26] Kløverpris et al[27] used SPR biosensors to analyze stanniocalcin-1, which can potently inhibit the proteolytic activity of PAPP-A. In addition, Smith et al[28] used SPR methods and Western blots to investigate PAPP-A-resistant IGFBP-4, which has been shown to inhibit angiogenesis and metastasis of breast cancer in murine models.

With regards to PAPP-A2, Bocková et al[29] were the first to use SPR biosensors with functionalized gold nanoparticles to detect PAPPA-2 in blood plasma. They also measured PAPP-A2 with an SPR biosensor in long-term hemodialysis patients, and found that PAPP-A2 was increased in these patients.[4] In our previous study, we further demonstrated that a functionalized GO-based SPR biosensor had higher sensitivity, affinity and selective ability for PAPP-A2 than a traditional SPR biosensor.[30]

Figure 3 SPR sensorgrams of PAPP-A measurement.
Notes: (**A**) Assaying different concentrations of PAPP-A with the traditional SPR biosensor. (**B**) Assaying different concentrations of PAPP-A with the GO-SPR biosensor. The white background indicates the period before the antibody-antigen reaction, the blue background indicates the antibody-antigen association, and the pink background indicates the antibody-antigen dissociation.
Abbreviations: SPR, surface plasmon resonance; PAPP-A, pregnancy-associated plasma protein-A; GO, graphene oxide.
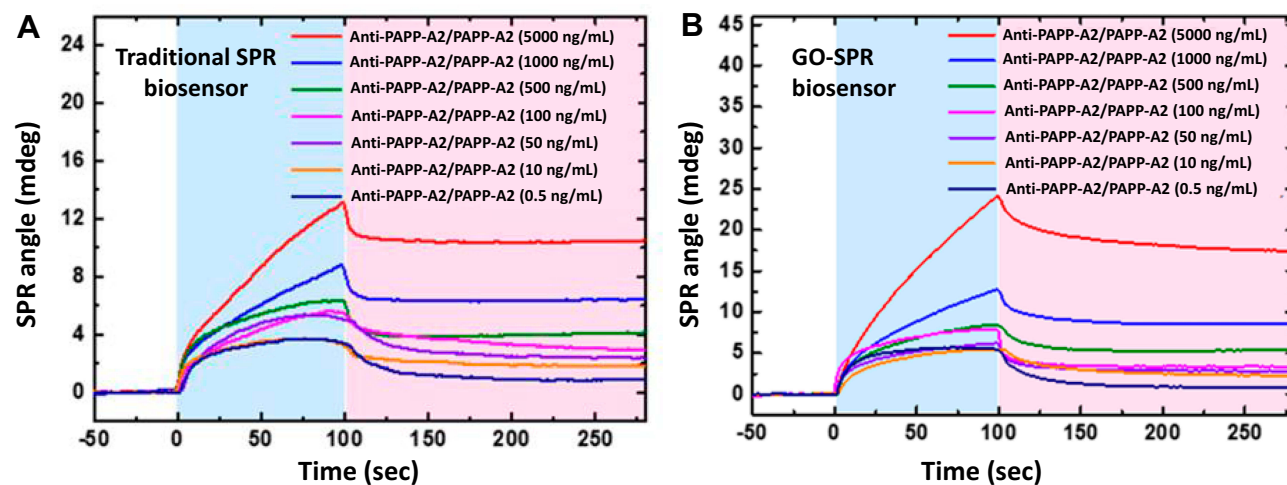
Figure 4 SPR sensorgrams of PAPP-A2 measurement.
Notes: (**A**) Assaying different concentrations of PAPP-A2 with the traditional SPR biosensor. (**B**) Assaying different concentrations of PAPP-A2 with the GO-SPR biosensor. The white background indicates the period before the antibody-antigen reaction, the blue background indicates the antibody-antigen association, and the pink background indicates the antibody-antigen dissociation.
Abbreviations: SPR, surface plasmon resonance; PAPP-A2, pregnancy-associated plasma protein-A2; GO, graphene oxide.

In this pilot study, we first used a GO-based SPR biosensor to simultaneously measure PAPP-A and PAPP-A2. The time from the beginning of antibody-antigen association to the end of antibody-antigen dissociation in both the traditional SPR and GO-SPR biosensors to detect PAPP-A and PAPP-A2 took only about 150 seconds. However, comparing the immunoassay sensitivity of both biosensors revealed that the GO-SPR biosensor was more sensitive at higher concentrations of PAPP-A or PAPP-A2,

within certain limits, than the traditional SPR biosensor according to SPR angle shift.

In the configuration of a traditional SPR biosensor, a thin metal film (such as gold in our study) is applied on a prism to support SPP propagation in the visible light spectrum. Gold is steady and resistant to oxidation, but not excellent at absorbing biomarkers, which restricts the sensitivity of traditional SPR biosensors. The special properties of GO-SPR biosensors allow for greater changes in the

Table 1 Studies of SPR Biosensors for PAPP-A or PAPP-A2 Measurements

Author	Biomarker	Application
Mikkelsen et al[25]	PAPP-A	Binding of PAC1 to PAPP-A in the presence of calcium ions
Mikkelsen et al[26]	PAPP-A	Investigation of interaction between PAPP-A and recombinant antibodies in animal species
Kløverpris et al[27]	PAPP-A	Inhibition of the proteolytic activity of PAPP-A by stanniocalcin-1
Smith et al[28]	PAPP-A	Inhibition of angiogenesis and metastasis of breast cancer by PAPP-A resistant IGFBP-4 in murine models
Bocková et al[29]	PAPP-A2	Detection of PAPP-A2 in blood plasma by SPR biosensors with functionalized gold nanoparticles
Kalousová et al[4]	PAPP-A2	Detection of PAPP-A2 in blood plasma of hemodialysis patients
Chiu et al[30]	PAPP-A2	Detection of PAPP-A2 in blood plasma by SPR biosensors with functionalized graphene oxide

Abbreviations: SPR, surface plasmon resonance; PAPP-A, pregnancy-associated plasma protein-A; PAPP-A2, pregnancy-associated plasma protein-A2; PAC1, pituitary adenylate cyclase-activating polypeptide type 1; IGFBP-4, insulin-like growth factor binding protein-4.

refractive index at the sensing medium interface compared to traditional SPR biosensors. Furthermore, coating the gold surface with GO will modify the propagation constant of SPP, which thereby changes the sensitivity to changes in the refractive index. In addition, modifying the oxygen-containing functional groups on the GO surface can increase its bandgap and dielectric constant, which also improve the GO-SPR properties.[19] Our experimental results showed the advantages of real-time detection and high sensitivity of GO-SPR biosensors.

Real-Time Detection of PAPP-a and PAPP-A2 in Mixed Interference Protein Samples with the GO-SPR Biosensor

Figure 5 shows the results of assaying PAPP-A and PAPP-A2 in samples with mixed interference proteins (CK-19, HSA, hCG, and CA 19–9) using the GO-SPR biosensor. The SPR angle shifts for PAPP-A at concentrations of 5000, 1000,

500, 100, 50, 10, and 0.5 ng/mL were 19.17, 13.35, 7.11, 5.70, 4.73, 3.83 and 2.28 mdegs, respectively (Figure 5A), compared to 17.51, 13.86, 11.56, 6.07, 4.03, 4.00, and 1.43 mdegs, respectively, for PAPP-A2 (Figure 5B).

Comparing Figure 5A (mixed proteins) with Figure 3B (PAPP-A alone), the major differences in SPR responses occurred during the antibody-antigen association (the blue background), but the SPR responses were similar after the antibody-antigen dissociation (the pink background). The higher SPR responses during the antibody-antigen association resulted from high concentrations of the whole antigens and non-specific interactions between anti-PAPP-A antibodies and mixed interference proteins. After the antibody-antigen dissociation, most of the mixed interference proteins were removed, resulting in comparable SPR angle shifts between PAPP-A alone and mixed protein measurements when the experiment had finished. The same phenomenon was noted between Figures 5B and 4B for PAPP-A2 detection. These
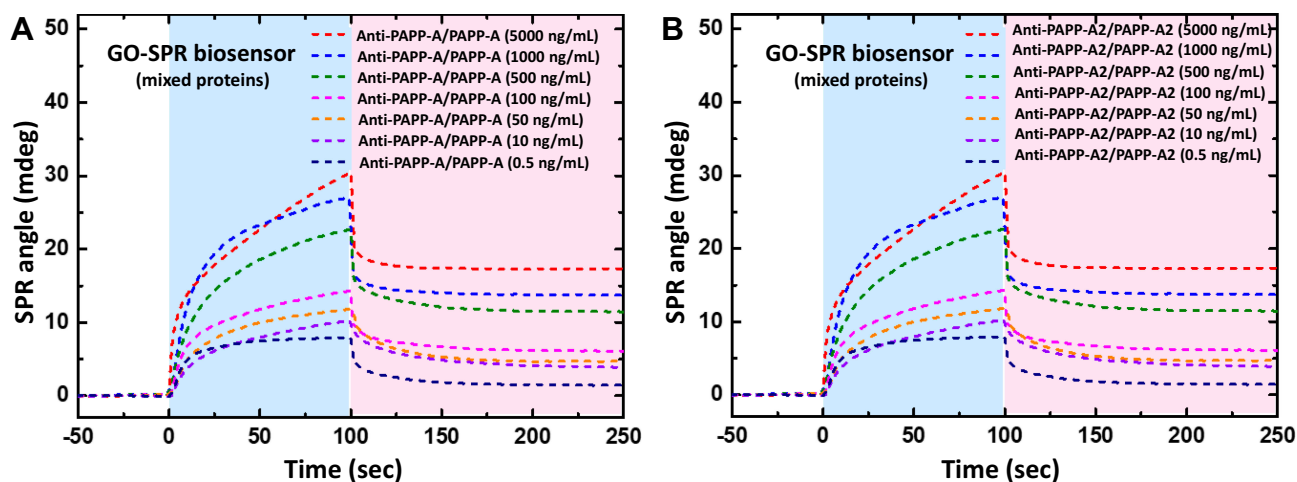
Figure 5 SPR sensorgrams of assaying different concentrations of PAPP-A (**A**) and PAPP-A2 (**B**) with mixed interference proteins with the GO-SPR biosensor.
Notes: The white background indicates the period before the antibody-antigen reaction, the blue background indicates the antibody-antigen association, and the pink background indicates the antibody-antigen dissociation.
Abbreviations: SPR, surface plasmon resonance; PAPP-A, pregnancy-associated plasma protein-A; PAPP-A2, pregnancy-associated plasma protein-A2; GO, graphene oxide.

results revealed the excellent specificity and binding affinity of the GO-SPR biosensor for PAPP-A and PAPP-A2 measurements. The superior high specificity and affinity indicate that the GO-SPR biosensor could be used to analyze clinical blood samples of high-risk pregnant women.

SPR Response Curves of the Traditional SPR Biosensor and GO-SPR Biosensor

Figure 6 shows the SPR response curves and curve-fitting equations of PAPP-A and PAPP-A2 measurements with the traditional SPR and GO-SPR biosensors, where X is the concentration of PAPP-A or PAPP-A2, and Y is the SPR angle (mdeg). For PAPP-A, the calibration curves were fitted by $Y = 9.858–7.487 \, e^{-1.111x}$ (correlation coefficient (R^2) = 0.81) for the traditional SPR biosensor, $Y = 18.21–15.46 \, e^{-1.35x}$ ($R^2 = 0.96$) for the GO-SPR biosensor (PAPP-A alone), and $Y = 17.155–14.251 \, e^{-1.758x}$ ($R^2 = 0.97$) for the GO-SPR biosensor (mixed proteins). For PAPP-A2, the calibration curves were fitted by $Y = 10.701–8.952 \, e^{-0.719x}$ ($R^2 = 0.97$) for the traditional SPR biosensor, $Y = 17.847–16.324 \, e^{-0.942x}$ ($R^2 = 0.94$) for the GO-SPR biosensor (PAPP-A2 alone), and $Y = 19.554–16.122 \, e^{-0.807x}$ ($R^2 = 0.95$) for the GO-SPR biosensor (mixed proteins). Both the experimental data of the traditional SPR biosensor and GO-SPR biosensor were highly consistent with the calibration curves.
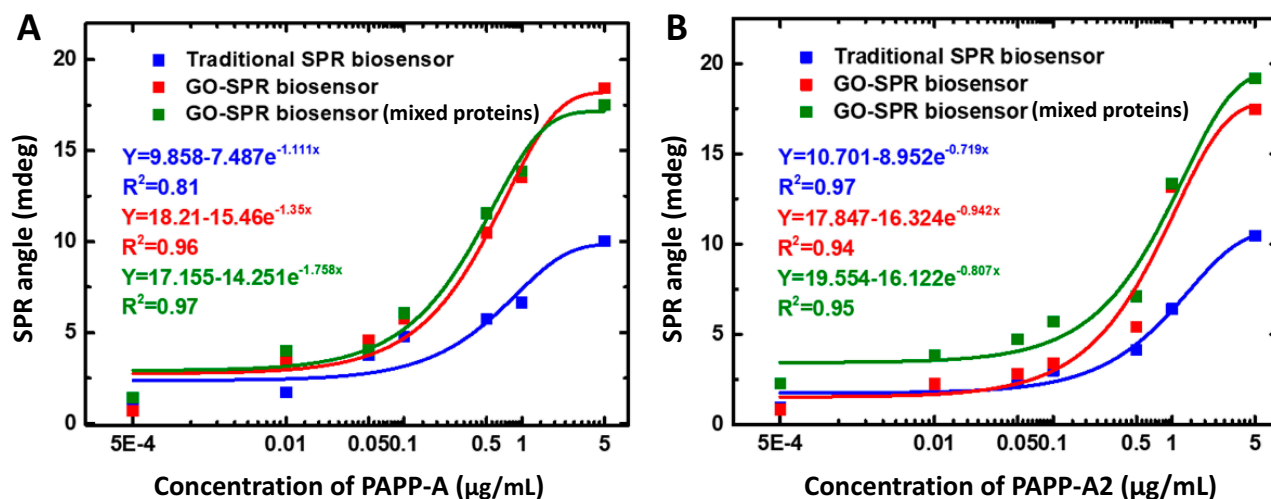
Compared with the traditional SPR biosensor, the GO-SPR biosensor had a higher sensitivity. In addition, the SPR angle shifts with the GO-SPR biosensor were nearly double those of the traditional SPR biosensor at a concentration of PAPP-A and PAPP-A2 of 5 µg/mL. The limit of detection

(LOD) of the GO-SPR biosensor was as low as 0.5 ng/mL for both PAPP-A and PAPP-A2. Clinically, the concentrations of PAPP-A and PAPP-A2 in the first trimester of a normal pregnancy are about 610 ng/mL and 23 ng/mL, respectively, and they increase with gestational age.[9,32] Thus, the ideal LOD of the GO-SPR biosensors for PAPP-A and PAPP-A2 measurements was low enough to examine blood samples of pregnant women.

One drawback of this study is the LOD of the GO-SPR biosensor is not better than that of enzyme-linked immunosorbent assay (ELISA) (LOD 0.071 ng/mL).[33] However, in contrast to ELISA, the GO-SPR biosensor is real-time, label-free, fast, and low-cost. It can quantitatively measure biomarkers without the need for secondary antibodies to generate signals, and the LOD of the GO-SPR biosensors was low enough to measure clinical blood samples.

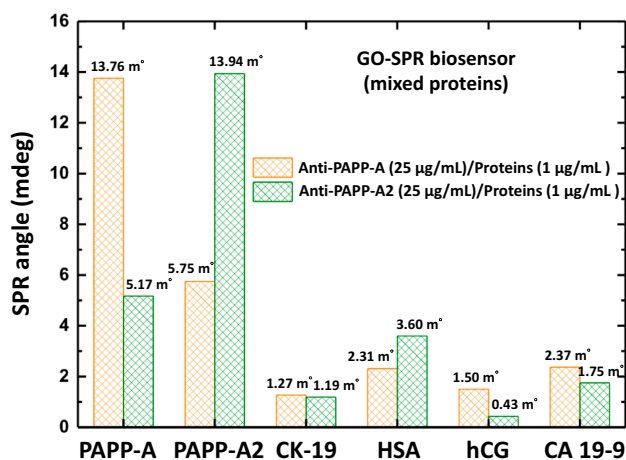## Interference Test and Specificity Analysis

Figure 7 shows the results of specificity assays of anti-PAPP -A and anti-PAPP-A2 at a concentration of 25 µg/mL with different proteins (CK-19, HSA, hCG, and CA 19–9) at a concentration of 1 µg/mL with the GO-SPR biosensor. It is important to consider SPR angle errors and deviations caused by nonspecific interference proteins. For the GO-SPR biosensor immobilized with anti-PAPP-A antibodies, the measured SPR angle shifts of PAPP-A, PAPP-A2, CK-19, HSA, hCG, and CA 19–9 were 13.76, 5.75, 1.27, 2.31, 1.50, and 2.37 mdegs, respectively, compared to 5.17, 13.94, 1.19, 3.60, 0.43, and 1.75 mdegs, respectively, for the GO-SPR biosensor immobilized with anti-PAPP-A2 antibodies.

Figure 6 SPR response curves and curve-fitting equations of PAPP-A (**A**) and PAPP-A2 (**B**) measurements with the traditional SPR biosensor and GO-SPR biosensor.
Notes: X represents the concentration of PAPP-A or PAPP-A2, and Y represents the SPR angle (mdeg).
Abbreviations: SPR, surface plasmon resonance; PAPP-A, pregnancy-associated plasma protein-A; PAPP-A2, pregnancy-associated plasma protein-A2; GO, graphene oxide.

Figure 7 Specificity assays of anti-PAPP-A or anti-PAPP-A2 at a concentration of 25 μg/mL in a mixture of different proteins (CK-19, HSA, hCG, and CA 19–9) at a concentration of 1 μg/mL with the GO-SPR biosensor.
Abbreviations: PAPP-A, pregnancy-associated plasma protein-A; PAPP-A2, pregnancy-associated plasma protein-A2; CK-19, cytokeratin 19; HSA, human serum albumin; hCG, human chorionic gonadotropin; CA 19–9, cancer antigen 19–9; GO, graphene oxide; SPR, surface plasmon resonance.

For the GO-SPR biosensor with anti-PAPP-A antibodies, almost all of the bonded protein from the mixture of proteins was PAPP-A, and almost no other proteins were captured except for PAPP-A2, which had the second strongest signal resulting from a slight antibody-antigen reaction with anti-PAPP-A. However, the SPR signal of PAPP-A2 (5.75 mdeg) was much smaller than that of PAPP-A (13.76 mdeg). Similar experimental results were noted for the GO-SPR biosensor with anti-PAPP-A2 antibodies, and most of the bonded protein was PAPP-A2. The SPR signal of PAPP-A (5.17 mdeg) was much smaller than that of PAPP-A2 (13.94 mdeg). These results suggested that adding mixed interference proteins did not have a significant effect on PAPP-A or PAPP-A2 measurements.

PAPP-A and PAPP-A2 are the only two members of the pappalysin family of metalloproteinases, and they share 45% amino acid sequence homology with each other.[3] Both participate in regulating the IGF system through complex interactions, resulting in slight antibody-antigen responses of anti-PAPP-A/PAPP-A2 and anti-PAPP-A2/PAPP-A. According to the large disparity in SPR responses, the GO-SPR biosensor had high specificity to distinguish PAPP-A and PAPP-A2 in a complex environment with many mixed interference proteins.

The human body fluid is a complicated biological fluid containing numerous proteins and other materials that may cause lower sensitivity of SPR compared to that in the buffer solution. Although our work pointed out that both

PAPP-A and PAPP-A2 could be detected in the more than 50-fold dilution samples, implying that this biosensor could selectively detect targets in clinical samples with a simple dilution step, measurement of PAPP-A and PAPP-A2 in undiluted and unprocessed serum is still a goal for our team to achieve.

Conclusion

In this study, we verified the potential of a GO-SPR biosensor to simultaneously measure PAPP-A and PAPP-A2. Both PAPP-A and PAPP-A2 are valuable biomarkers for pregnancy-associated diseases such as fetal Down syndrome, low birth weight, preterm delivery, and maternal preeclampsia. Low birth rates and an aging population are global concerns, and the issue of improved screening for the complications of pregnancy remains a priority to decrease maternal and perinatal morbidity and mortality. PAPP-A and PAPP-A2 have intricate interactions and an inverse association with each other. From this point of view, developing a novel immunoassay technique to measure and differentiate PAPP-A and PAPP-A2 simultaneously may aid in the differential diagnosis of pregnancy-associated diseases.

Our findings suggest that GO-SPR biosensors may be a promising tool to distinguish PAPP-A and PAPP-A2 under a complex environment with various mixed interference proteins such as in clinical blood samples during pregnancy. The advantages of a GO-SPR biosensor include high sensitivity, high specificity, easy operation, real-time measurements, and low cost. Moreover, GO-SPR biosensors appear to be particularly well suited to meet the growing demand for biosensors in point-of-care testing.

Acknowledgments

Disclosure

The authors report no conflicts of interest in this work.

References

1. Boldt HB, Overgaard MT, Laursen LS, et al. Mutational analysis of the proteolytic domain of pregnancy-associated plasma protein-A (PAPP-A): classification as a metzincin. *Biochem J.* 2001;358 (2):359–367. doi:10.1042/bj3580359
2. Boldt HB, Conover CA. Pregnancy-associated plasma protein-A (PAPP-A): a local regulator of IGF bioavailability through cleavage of IGFBPs. *Growth Horm IGF Res.* 2007;17(1):10–18. doi:10.1016/j. ghir.2006.11.003

3. Overgaard MT, Boldt HB, Laursen LS, et al. Pregnancy-associated plasma protein-A2 (PAPP-A2), a novel insulin-like growth factor-binding protein-5 proteinase. *J Biol Chem*. 2001;276 (24):21849–21853. doi:10.1074/jbc.M102191200

4. Kalousová M, Dusilová-Sulková S, Kuběna AA, et al. Pregnancy-associated plasma protein A2 in hemodialysis patients: significance for prognosis. *Kidney Blood Press Res*. 2017;42(3):509–518. doi:10.1159/000479847

5. Agrogiannis GD, Sifakis S, Patsouris ES, et al. Insulin-like growth factors in embryonic and fetal growth and skeletal development (Review). *Mol Med Rep*. 2014;10(2):579–584. doi:10.3892/mmr.2014.2258

6. Hourrier S, Salomon LJ, Dreux S, et al. Screening for adverse pregnancy outcome at early gestational age. *Clin Chim Acta*. 2010;411(21–22):1547–1552. doi:10.1016/j.cca.2010.06.024

7. Kalousová M, Muravská A, Zima T. Pregnancy-associated plasma protein A (PAPP-A) and preeclampsia. *Adv Clin Chem*. 2014;63:169–209.

8. Munnangi S, Gross SJ, Mudankamar R, et al. Pregnancy associated plasma protein-A2: a novel biomarker for down syndrome. *Placenta*. 2014;35(11):900–906. doi:10.1016/j.placenta.2014.08.001

9. Crosley EJ, Durland U, Seethram K, et al. First-trimester levels of pregnancy-associated plasma protein A2 (PAPP-A2) in the maternal circulation are elevated in pregnancies that subsequently develop preeclampsia. *Reprod Sci*. 2014;21(6):754–760. doi:10.1177/1933719113512532

10. Macintire K, Tuohey L, Ye L, et al. PAPPA2 is increased in severe early onset pre-eclampsia and upregulated with hypoxia. *Reprod Fertil Dev*. 2014;26(2):351–357. doi:10.1071/RD12384

11. DiPrisco B, Kumar A, Kalra B, et al. Placental proteases PAPP-A and PAPP-A2, the binding proteins they cleave (IGFBP-4 and −5), and IGF-I and IGF-II: levels in umbilical cord blood and associations with birth weight and length. *Metabolism*. 2019;100:153959. doi:10.1016/j.metabol.2019.153959;.

12. Roh S, Chung T, Lee B. Overview of the characteristics of micro- and nano-structured surface plasmon resonance sensors. *Sensors*. 2011;11 (2):1565–1588. doi:10.3390/s110201565

13. Chang CC, Chiu NF, Lin DS, et al. High-sensitivity detection of carbohydrate antigen 15-3 using a gold/zinc oxide thin film surface plasmon resonance-based biosensor. *Anal Chem*. 2010;82 (4):1207–1212. doi:10.1021/ac901797j

14. Chang CC, Lin S, Wei SC, et al. An amplified surface plasmon resonance "turn-on" sensor for mercury ion using gold nanoparticles. *Biosens Bioelectron*. 2011;30(1):235–240. doi:10.1016/j.bios.2011.09.018

15. Chen CY, Chang CC, Yu C, et al. Clinical application of surface plasmon resonance-based biosensors for fetal fibronectin detection. *Sensors*. 2012;12(4):3879–3890. doi:10.3390/s120403879

16. Zhang Y, Wang G, Yang L, et al. Recent advances in gold nanostructures based biosensing and bioimaging. *Coord Chem Rev*. 2018;370:1–21. doi:10.1016/j.ccr.2018.05.005

17. Liu A, Wang G, Wang F, et al. Gold nanostructures with near-infrared plasmonic resonance: synthesis and surface functionalization. *Coord Chem Rev*. 2017;336:28–42. doi:10.1016/j.ccr.2016.12.019

18. Wu L, Chu HS, Koh WS, et al. Highly sensitive graphene biosensors based on surface plasmon resonance. *Opt Express*. 2010;18 (14):14395–14400. doi:10.1364/OE.18.014395

19. Chiu NF, Huang TY, Lai HC, et al. Graphene oxide-based SPR biosensor chip for immunoassay applications. *Nanoscale Res Lett*. 2014;9(1):1–7. doi:10.1186/1556-276X-9-445

20. Chiu NF, Kuo CT, Lin TL, et al. Ultra-high sensitivity of the non-immunological affinity of graphene oxide-peptide-based surface plasmon resonance biosensors to detect human chorionic gonadotropin. *Biosens Bioelectron*. 2017;94:351–357. doi:10.1016/j.bios.2017.03.008

21. Chiu NF, Fan SY, Yang CD, et al. Carboxyl-functionalized graphene oxide composites as SPR biosensors with enhanced sensitivity for immunoaffinity detection. *Biosens Bioelectron*. 2017;89:370–376. doi:10.1016/j.bios.2016.06.073

22. Ramdzan NSM, Fen YW, Omar NAS, et al. Optical and surface plasmon resonance sensing properties for chitosan/carboxyl-functionalized graphene quantum dots thin film. *Optik*. 2019;17:802–812. doi:10.1016/j.ijleo.2018.10.071

23. Stankovich S, Dikin DA, Dommett GH, et al. Graphene-based composite materials. *Nature*. 2006;442(7100):282–286. doi:10.1038/nature04969

24. Chung C, Kim YK, Shin D, et al. Biomedical applications of graphene and graphene oxide. *Acc Chem Res*. 2013;46(10):2211–2224. doi:10.1021/ar300159f

25. Mikkelsen JH, Gyrup C, Kristensen P, et al. Inhibition of the proteolytic activity of pregnancy-associated plasma protein-A by targeting substrate exosite binding. *J Biol Chem*. 2008;283(24):16772–16780. doi:10.1074/jbc.M802429200

26. Mikkelsen JH, Steffensen LB, Oxvig C. Development of a recombinant antibody towards PAPP-A for immunohistochemical use in multiple animal species. *J Immunol Methods*. 2014;404:33–40. doi:10.1016/j.jim.2013.12.002

27. Kløverpris S, Mikkelsen JH, Pedersen JH, et al. Stanniocalcin-1 potently inhibits the proteolytic activity of the metalloproteinase pregnancy-associated plasma protein-A. *J Biol Chem*. 2015;290 (36):21915–21924. doi:10.1074/jbc.M115.650143

28. Smith YE, Toomey S, Napoletano S, et al. Recombinant PAPP-A resistant insulin-like growth factor binding protein 4 (dBP4) inhibits angiogenesis and metastasis in a murine model of breast cancer. *BMC Cancer*. 2018;18(1):1016. doi:10.1186/s12885-018-4950-0

29. Bocková M, Chadtová Song X, Gedeonová E, et al. Surface plasmon resonance biosensor for detection of pregnancy associated plasma protein A2 in clinical samples. *Anal Bioanal Chem*. 2016;408 (26):7265–7269. doi:10.1007/s00216-016-9664-z

30. Chiu NF, Tai MJ, Wu HP, et al. Development of a bioaffinity SPR immunosensor based on functionalized graphene oxide for the detection of pregnancy-associated plasma protein A2 in human plasma. *Int J Nanomedicine*. 2019;14:6735–6748. doi:10.2147/IJN

31. Fischer MJ. Amine coupling through EDC/NHS: a practical approach. *Methods Mol Biol*. 2010;627:55–73.

32. Bischof P, DuBerg S, Herrmann W, et al. Pregnancy-associated plasma protein-A (PAPP-A) and hCG in early pregnancy. *Br J Obstet Gynaecol*. 1981;88(10):973–975. doi:10.1111/bjo.1981.88.issue-10

33. Kloverpris S, Gaidamauskas E, Rasmussen LCV, et al. A robust immunoassay for pregnancy-associated plasma protein-A2 based on analysis of circulating antigen: establishment of normal ranges in pregnancy. *Mol Hum Reprod*. 2013;19:756–763. doi:10.1093/molehr/gat047